Proceedings Paper:

Gadelovits, S., Zhong, Q.C., Konstantopoulos, G.C. orcid.org/0000-0003-3339-6921 et al. (1 more author) (2017) Design of a UDE Frequency Selective Filter to Reject Periodical Disturbances. In: IFAC-PapersOnLine. 20th IFAC World Congress, 09 Jul - 14 Sep 2017, Toulouse, France. Elsevier , pp. 7824-7829.

https://doi.org/10.1016/j.ifacol.2017.08.1059

Design of a UDE Frequency Selective Filter to Reject Periodical Disturbances

Shlomo Gadelovits * **Qing-Chang Zhong** ** **George C. Konstantopoulos** * **Visakan Kadirkamanathan** *

* *Department of Automatic Control and Systems Engineering The University of Sheffield, Sheffield, S1 3JD, UK s.gadelovits@sheffield.ac.uk*
** *Department of Electrical and Computer Engineering Illinois Institute of Technology, Chicago, IL 60616, USA zhongqc@ieee.org*

Abstract: In this paper a new filter design for the Uncertainty and Disturbance Estimator (UDE) is proposed to reject periodical disturbances when a limited bandwidth is required for the control output. The motivation comes from several applications where the system actuator may introduce a bandwidth limitation, as a result of internal delays, or when the actuator itself is a limited bandwidth closed-loop system. When the traditional UDE approach is applied in these systems, the stability requirements impose a limitation over the effective bandwidth of the UDE filter and therefore disturbances cannot be fully rejected by the filter. In the case where the expected disturbance is periodical with a known fundamental frequency, the proposed UDE filter is designed as a chain of filters to match selected bands of the expected disturbance spectrum and fully reject them while maintaining the desired stability margins. A design example of a power inverter application is investigated and extensive simulation results are provided to verify the proposed UDE filter design.

Keywords: Uncertainty and disturbance estimator, disturbance rejection, limited bandwidth design, power systems, stability margins.

1. INTRODUCTION

The UDE control theory was first proposed in (Zhong and Rees, 2004) to achieve disturbance rejection of a system with uncertainties and external disturbances. This theory has been evolved from the time delay control problem, which has been investigated in (Youcef-Toumi and Ito, 1987, 1990), to overcome the need of calculating derivatives of system states and to cancel the need of a delay in the controller. Successful applications of the UDE approach include several practical examples, such as servo control (Ren et al., 2017), wind turbine control, (Ren and Zhong, 2013), inverter power flow control (Wang et al., 2016) and DC-DC voltage regulation (Kuperman, 2013).

One of the crucial stages in the implementation of the UDE controller is the design of the UDE filter (Kuperman et al., 2010), since the filter design plays a key role in the disturbance rejection performance. In the literature, several types of low-pass filters (LPFs) have been proposed for UDE controllers such as first-order filters (Kuperman et al., 2010), high-order filters (Shendge and Patre, 2007), the α-filter (Chandar and Talole, 2014), etc, to further improve the disturbance rejection. These methods provide very good results when either the disturbance is constant or when the disturbance spectrum is clearly inside the UDE filter bandwidth. However, in many applications, the actuator bandwidth is limited due to the sampling frequency or due to the actuator's internal structure, which imposes a bandwidth limitation for the UDE filter design (Kuperman, 2015) and therefore the LPF design may result in a degraded performance. In addition, in the case where the plant model is not given in the canonic form, a cascaded multi-loop structure has to be applied in order to comply with the UDE constraint that is related to the calculation of a pseudo-inverse matrix, as described in (Zhong and Rees, 2004). In the case of a multiloop control architecture when the expected disturbance is in the low frequency range, the control loops can be decoupled in the frequency domain by limiting the outer loop bandwidth to a lower decade (Maffezzoni et al., 1990). However, in applications that include voltage or current regulation of an inverter stage (Gouraud et al., 1997; Rioual et al., 1996), rotational machinery speed, torque or position regulation (Tomizuka, 2008), the expected disturbance is periodical and may contain a known harmonic spectrum. Hence, if the disturbance harmonic content is not clearly inside the UDE filter bandwidth, it will not be attenuated completely. Nevertheless, when the UDE filter is designed as LPF, the transfer function of the disturbance to the output reaches a peak gain around the geometric average of the reference model and the UDE filter bandwidths.

In this paper a new approach to the UDE filter design is proposed. In this approach, the UDE filter is designed as a Frequency Selective Filter (FSF) where each expected disturbance harmonic is attenuated by the filter without violating the bandwidth limitations. It is shown in the paper that the suitable filter design is achieved by selecting the desired disturbance rejection function. A design example of an inverter output voltage regulation is presented where the inverter is driven by a limited bandwidth current regulator. Simulation results of the inverter connected to nonlinear load are provided to validate the theory and a comparison between the proposed FSF and the LPF methods is presented.

The paper is organized as follows: Section 2 provides an overview of the UDE approach. The proposed design for the UDE filter is presented in Section 3, where it is explained how the periodical disturbance is rejected. A practical example of an inverter application is investigated in Section 4 and extensive simulation results are provided to verify the effectiveness of the proposed method. Finally, in Section 5, some conclusions are drawn.

2. OVERVIEW OF THE UDE-BASED APPROACH

Consider a linear time-invariant single-input-single-output system of the form

$$\dot{x}(t) = (A + \Delta A(t))x(t) + (B + \Delta B(t))u(t) + d(t), \quad (1)$$

where ΔA, ΔB represent the system uncertainties and $d(t)$ is an unmeasurable disturbance. The main task is to track a reference signal independently from the system uncertainties or the external disturbance. Hence, a reference model is designed as

$$\dot{x}_m(t) = A_m x_m(t) + B_m r(t), \quad (2)$$

where $r(t)$ is the desired reference and A_m, B_m are the state-space matrices of the desired dynamics. Consider the error vector

$$e(t) = \begin{bmatrix} x_{m1} - x_1 \\ x_{m2} - x_2 \\ \cdots\cdot \\ x_{mn} - x_n \end{bmatrix} \quad (3)$$

where n is the system order. Then the main challenge is to find a control law which guarantees closed-loop stability for the error dynamics

$$\dot{e}(t) = A_m e(t). \quad (4)$$

Based on the UDE approach (Kuperman et al., 2010), such a controller takes the form

$$u(t) = B^+(A_m x(t) + B_m r(t) - Ax(t) - ude(t)), \quad (5)$$

where $B^+ = (B^T B)^{-1} B^T$ is the pseudo inverse of B. The term $ude(t)$ is calculated from the system uncertainties and disturbances as

$$ude(t) = u_d(t) \star g(t), \quad (6)$$

where $g(t)$ is the impulse response of the UDE filter, $'\star'$ is the convolution operator and $u_d(t)$ is the calculated disturbances and uncertainties. The term $u_d(t)$ is obtained from (1) as

$$u_d(t) = \Delta A(t)x(t) + \Delta B(t)u(t) + d(t) = \dot{x}(t) - Ax - Bu. \quad (7)$$

It is worth noting that the UDE solution includes a pseudo-inverse term and therefore the constraint

$$[I - BB^+] \cdot [A_m x + B_m r(t) - Ax - \Delta A(t)x - d(t)] = 0 \quad (8)$$

must be met (Zhong and Rees, 2004). According to the analysis in (Zhong et al., 2011), the state dynamics of the UDE-controlled system becomes

$$X(s) = H_m(s)R(s) + H_d(s)B \cdot B^+ U_d(s), \quad (9)$$

where

$$H_m(s) = (sI - A_m)^{-1} B_m \quad (10)$$

and

$$H_d(s) = (sI - A_m)^{-1}(1 - G(s)). \quad (11)$$

From (11) there is $H_d(s) = H_k(s)H_f(s)$ with $H_k(s) = (sI - A_m)^{-1}$ and $H_f(s) = (1 - G(s))$. Combining (5), (7) and (6), yields the UDE-based control law

$$u(t) = -B^+ \left(Ax(t) + L^{-1}\left\{ \frac{sG(s)}{1 - G(s)} \right\} \star x(t) - \right.$$
$$\left. - L^{-1}\left\{ \frac{1}{1 - G(s)} \right\} \star (A_m x(t) + B_m r(t)) \right), \quad (12)$$

where $L^{-1}\{\cdot\}$ the inverse Laplace operator. Note here that the reference model should be chosen in accordance to the desired tracking bandwidth and transient performance.

3. PROPOSED UDE FILTER TO REJECT PERIODICAL DISTURBANCE

Consider a plant system of the form of (1) operated by an actuator with a maximum actuator input bandwidth of ω_{max}. Given that the UDE approach, described in the previous section, is applied to this system in order to follow a reference model, the control signal u has to satisfy the bandwidth requirement. Therefore

$$|U(j\omega)| < \frac{1}{\sqrt{2}}, \in \omega > \omega_{max}. \quad (13)$$

From (12), the Laplace form of $u(t)$ after rearranging the terms becomes

$$U(s) = \underbrace{B^+ \left(\frac{1}{1 - G} \right) B_m}_{H_{FF}(s)} R(s) -$$
$$- \underbrace{\left(B^+ A - \frac{1}{1 - G} \cdot B^+ A_m + B^+ \frac{sG}{1 - G} \right)}_{H_{FB}(s)} X(s) \quad (14)$$

where $H_{FF}(s)$ is the feedforward term and $H_{FB}(s)$ is the feedback. Fig. 1 shows the equivalent control loop where $T(s)$ is the actuator transfer function, $P(s)$ is the plant model and $D(s)$ is the disturbance and uncertainty in the input. Looking at Fig. 1, the corresponding loop gain is

$$L(s) = H_{FB}(s) \cdot T(s) \cdot P(s). \quad (15)$$

To ensure closed-loop system stability, the loop-gain has to meet the minimum stability margins.

Additionally, according to (11), the dynamics of the disturbance are affected both by the choice of the reference model and by the design of the UDE filter. In (Zhong et al., 2011) it is proven that $u_d(t)$ is attenuated twice, since at the low frequency range it is attenuated by $H_f(s)$ and at

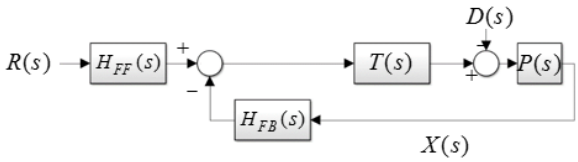

Figure 1. Equivalent loop diagram

the high frequency range by $H_k(s)$, as shown at Fig. 2. It is clear from (11) that when $G(s)$ equals to unity the disturbance is fully rejected. However, the main trade-off in the filter design is between performance and control signal bandwidth (Kuperman, 2015). By increasing the UDE filter bandwidth, the bandwidth of the UDE control signal u increases which eventually decreases the stability margins of the system.

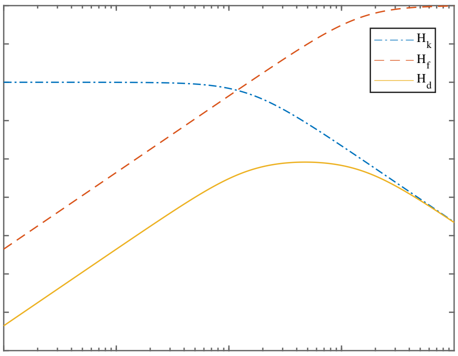

Figure 2. Sketch of low pass filter design

Hence, the main task is to design the UDE filter accordingly in order to reject the disturbance under a limited bandwidth of the control signal and guarantee the desired stability margins. In this paper, a periodical disturbance $d(t)$ that appears in the n harmonics of the rated frequency ω is considered , i.e.

$$d(t) = \sum_{i=1}^{n} d_i \sin(i\omega t + \theta_i). \tag{16}$$

In order to reject this disturbance, the proposed filter $H_f(s)$ is designed as a chain of Butterworth band stop filters of the form

$$N_i(s) = \frac{s^2 + \omega_H \cdot \omega_L}{s^2 + (\omega_H - \omega_L)s + \omega_H \cdot \omega_L}, \tag{17}$$

where ω_H and ω_L are the high and low limit of the stop band, respectively. The filter $H_f(s)$ is then calculated as the product of (17) as follows

$$H_f(s) = \prod_{i=1}^{n} N_i(s). \tag{18}$$

In order to guarantee the input bandwidth requirement, as a rule of thumb, the frequency ω_H of the $n-th$ band stop filter should be less than ω_{max}. Then, the resulted UDE filter is obtained from $H_f(s)$ as

$$G(s) = 1 - H_f(s) \tag{19}$$

The resulted filter $H_f(s)$ is illustrated in Fig. 3 for the first seven harmonics, which are considered to be inside the bandwidth of the control signal. The resulting Bode diagram of the Frequency Selective Filter (FSF) $G(s)$ is shown in Fig. 4. It is observed that the filter reaches a unity gain and zero phase at the desired frequencies. This results in $H_d(s) \to 0$ at the disturbance signal harmonics which leads to a clear rejection of the periodical disturbance.

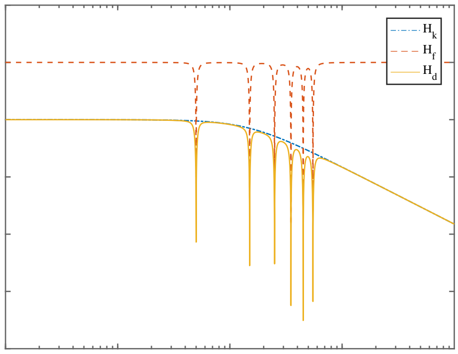

Figure 3. Sketch of the frequency selective filter design

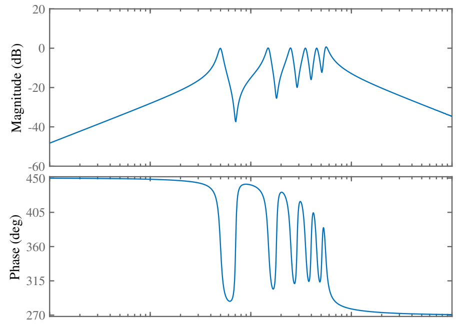

Figure 4. Frequency selective filter $G(s)$

4. DESIGN EXAMPLE

4.1 Power inverter output voltage regulator

Consider an AC inverter leg followed by an LC filter as shown in Fig. 5, where u_o is the inverter voltage that represents the control input, i_L is the inductor current, v_o is the output voltage and i_o is the load current. The parasitic resistances of the capacitor and the inductor are neglected for brevity. The inverter is connected to a load and the main task is for the inverter output voltage v_o to track the reference signal

$$r(t) = V_M \sin(\omega_0 t), \tag{20}$$

independently from the load disturbances, i.e. to reject linear and nonlinear periodical loads. This represents a common scenario in inverter applications where the load voltage should be equal to $r(t)$ by rejecting additional harmonic components that occur from the load dynamics.
Using Kirchoffs laws, the inverter model dynamics are given as

Table 1: Inverter parameters

Parameter	Value	Units
C	10	μF
ω_{max}	$2\pi \cdot 2000$	rad/s
ω_0	$2\pi \cdot 50$	rad/s

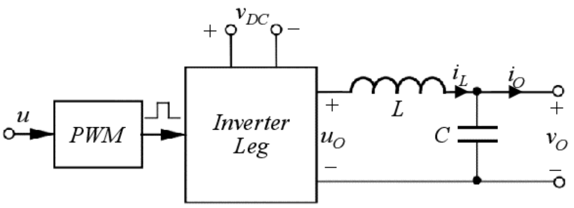

Figure 5. Schematic of a single-phase inverter with an output filter

$$L\frac{di_L}{dt} = u_o(t) - v_o(t) \tag{21}$$
$$C\frac{dv_o}{dt} = i_L(t) - i_o(t).$$

To comply with (8) and apply the UDE for the output voltage regulation, a cascaded control loop design is adopted. Hence, the dynamics (21) can be investigated only using the second equation

$$\frac{dv_o}{dt} = \frac{1}{C}i_L(t) - \frac{1}{C}i_o(t), \tag{22}$$

where $i_L(t)$ is the output of a closed loop inductor current regulator which serves as the actuator for the voltage dynamics (22) and $C^{-1}i_o(t)$ is the load current disturbance (see Fig. 6). Because of the PWM and digital control delay, the maximum allowed bandwidth of the current regulator reference $i_L^*(t)$ is limited by a defined ω_{max}. In many cases the closed loop current regulator can be approximated as first order LPF of the form

$$T_I(s) = \frac{\omega_{max}}{s + \omega_{max}}. \tag{23}$$

Following (22) it yields that

$$A = 0,\ B = C^{-1}$$

and $x \equiv v_o$. Given the reference signal $r(t)$ from (20), the

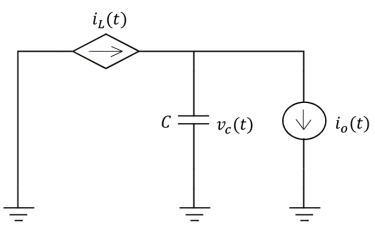

Figure 6. Equivalent circuit of output voltage dynamics

reference model dynamics are designed according to (2) as

$$\dot{x}_m(t) = -\omega_R x_m(t) + \omega_R r(t), \tag{24}$$

where ω_R is the bandwidth of the reference model and as a rule of thumb is chosen to be $\omega_R > 10\omega_0$ to ensure low tracking error. Note that (Ren et al., 2017) has recently proposed a design of the reference model for AC signal, to overcome the gap between the reference model output to the reference signal. The UDE control law is obtained from (12) as

$$I_L^*(s) = \frac{C}{1-G}(\omega_R(X(s) - R(s)) - sGX(s)). \tag{25}$$

Combining (15), (23), (25) and the Laplace transformation of (22), the loop gain results in

$$L_V(s) = \frac{\omega_R + sG(s)}{s(1-G(s))}T_I(s). \tag{26}$$

4.2 UDE filter design

The UDE filter is designed based on two requirements: i) meet the minimum stability margins and ii) reject the disturbances in the output within the relevant spectrum. In order to ensure stability, the UDE filter is designed for a minimum Phase Margin (PM) of 45^o and a minimum $6dB$ Gain Margin. Note from (22) that the disturbance is amplified by C^{-1} which is the inverse of the output capacitor size. In the presented inverter case, given the value of the capacitor, the disturbance is amplified by $100dB$. To verify the efficiency of the proposed FSF method, three different cases for the UDE filter are investigated: a) setting $G(s) = 0$, b) using a low-pass filter and c) using the proposed FSF.

Case 1: $G(s) = 0$

When the UDE filter is chosen to be $G(s) = 0$, the corresponding loop gain results from (23) and (26) in

$$L_V(s) = \frac{\omega_R}{s} \cdot \frac{\omega_{max}}{s + \omega_{max}}. \tag{27}$$

In this case the bandwidth of the reference model is maximized to the allowable stability margins and is set to $\omega_R = 2\pi \cdot 2800\,rad/s$. The left column of Fig. 7(a) shows the loop gain with the required stability margin and Fig. 7(b) shows the Bode diagram of the transfer function of the disturbance to the output voltage.

Case 2: Using a low-pass filter

In this case, the bandwidth of the reference model ω_R is set to be $2\pi \cdot 500\,rad/s$ in order to ensure suitable tracking. In order to demonstrate the trade-off between the filter design, two low pass filters with a different order (order-1 and order-2) are tested. The considered low pass filters are shown in Table 2. The middle column of Fig. 7(a) shows the loop gain of the cascaded system for the first and second-order filter. It is clear that by increasing the filter order, the cut-off frequency reduces and also the low-frequency disturbance rejection is improved. On the other hand, the use of a high order filter deteriorates the medium frequency disturbance rejection, as reflected from the middle column of Fig. 7(b).

Table 2: Tested Low Pass Filters

Order:	$G(s)$	ω_f
1	$\frac{\omega_f}{s+\omega_f}$	$2\pi \cdot 850$
2	$\frac{\frac{2}{\sqrt{2}}\omega_f+\omega_f^2}{s^2+\frac{2}{\sqrt{2}}\omega_f+\omega_f^2}$	$2\pi \cdot 350$

Case 3: Using the proposed FSF

As in the case for the low-pass filter, the bandwidth for the reference model is chosen to be $2\pi \cdot 500\,rad/s$. The design of the FSF filter begins by calculating the desired $H_f(s)$ as in Section 3. In the case of the inverter, in order to reduce the disturbance around the harmonics, the

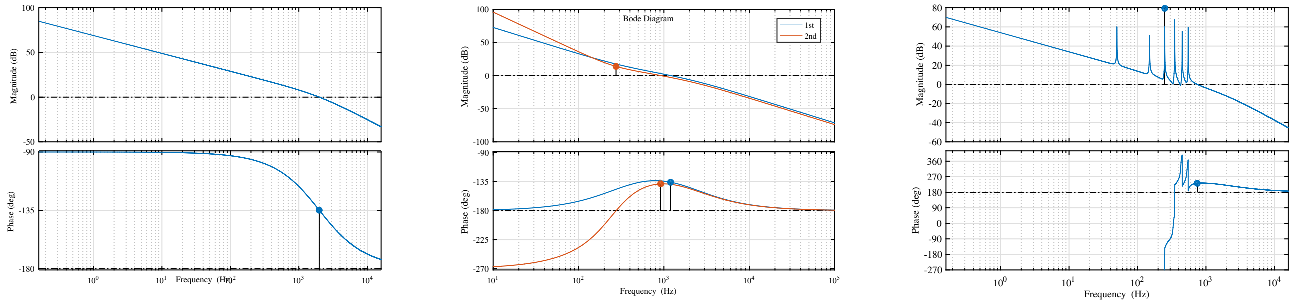

(a)

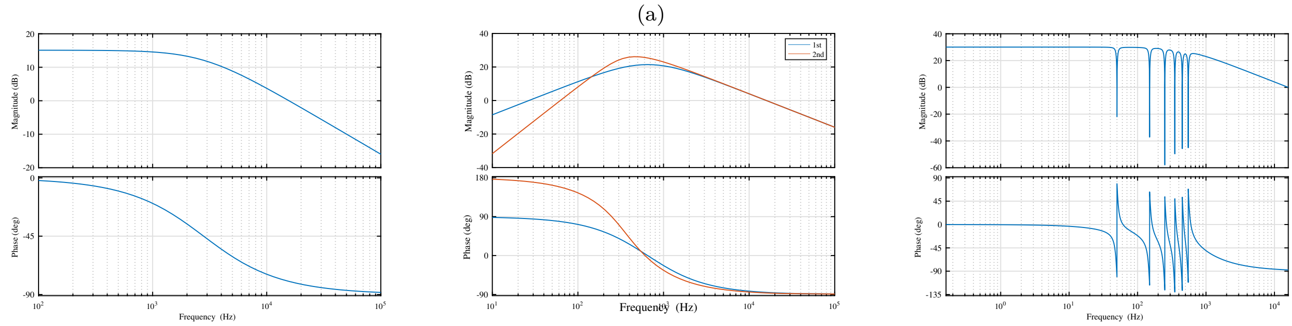

(b)

Figure 7. Bode Diagrams with $G(s) = 0$ (left column), 1st and 2nd order low-pass filters (middle column) and the proposed FSF (right column): (a) Loop-Gain and (b) Disturbance to output.

filter $H_f(s)$ has been calculated as a stop band around $50Hz$ and its odd harmonics up to the 11-th. The right column of Fig. 7(b) shows the disturbance to output bode where is is clearly shown the signal attenuation around the selected frequencies and Fig 7(a) reveals the loop gain Bode diagram of the cascaded system.

4.3 Simulation results

Simulation was carried out using the system presented in Section 4.1 connected to a nonlinear load, which consists of a diode rectifier connected to an RC load with $R_L = 50\Omega$ and $C_L = 570\mu F$. The reference voltage signal contains a single harmonic of $50Hz$ with amplitude of $155V$ having the form of (20). Fig. 8 shows the simulation results for the various filter designs. The left column of Fig. 8 shows the load current which is propotional to the system disturbance input ($d(t) = C^{-1}i_o(t)$). The middle column of Fig 8 shows the the error signal between the reference model output and the output voltage. The right column of Fig. 8 shows the spectrum of the output voltage where the harmonics are represented as a percentage of the fundamental component. It is observed that with the proposed FSF, all the harmonics of the output voltage up to the 11-th are completely attenuated opposed to the traditional low-pass filter design, thus significantly improving the total harmonic distortion of the output. In addtion the error signal $e(t)$ is significantly reduced thus without increasing the UDE filter bandwidth.

5. CONCLUSION

In this paper a new filter design for UDE controllers is revealed. It is shown that in a case where the actuator bandwidth is limited and the disturbance is expected to contain harmonics, it is better to design the UDE filter to match the unity value around the expected spectral content. The approach is investigated and compared to the traditional low pass filter design. Simulation results are provided to validate the theory.

REFERENCES

Chandar, T. and Talole, S. (2014). Improving the performance of ude-based controller using a new filter design. *Nonlinear Dynamics*, 77(3), 753–768.

Gouraud, T., Guglielmi, M., and Auger, F. (1997). Design of robust and frequency adaptive controllers for harmonic disturbance rejection in a single-phase power network. In *Control Conference (ECC), 1997 European*, 2605–2610. IEEE.

Kuperman, A., Zhong, Q.C., and Stobart, R. (2010). Filter design for UDE-based controllers. In *Proc. of Control 2010 UKACC Conference*.

Kuperman, A. (2013). UDE-based robust voltage control of dc-dc power converters. In *2013 5th International Congress on Ultra Modern Telecommunications and Control Systems and Workshops (ICUMT)*, 140–145. IEEE.

Kuperman, A. (2015). Design of alpha-filter-based UDE controllers considering finite control bandwidth. *Nonlinear Dynamics*, 81(1-2), 411–416.

Maffezzoni, C., Schiavoni, N., and Ferretti, G. (1990). Robust design of cascade control. *Control Systems Magazine, IEEE*, 10(1), 21–25.

Ren, B., Zhong, Q.C., and Dai, J. (2017). Asymptotic reference tracking and disturbance rejection of UDE-based robust control. *IEEE Trans. Ind. Electron.*, 64(4), 3166–3176. DOI 10.1109/TIE.2016.2633473.

Ren, B. and Zhong, Q.C. (2013). UDE-based robust control of variable-speed wind turbines. In *Industrial Electronics Society, IECON 2013-39th Annual Conference of the IEEE*, 3818–3823. IEEE.

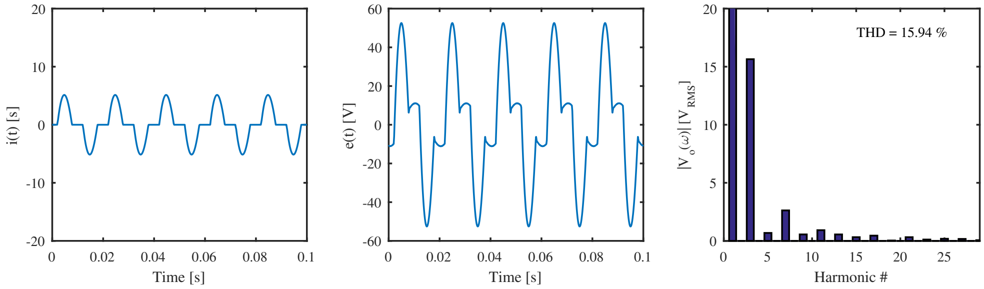

(a) $G(s) = 0$

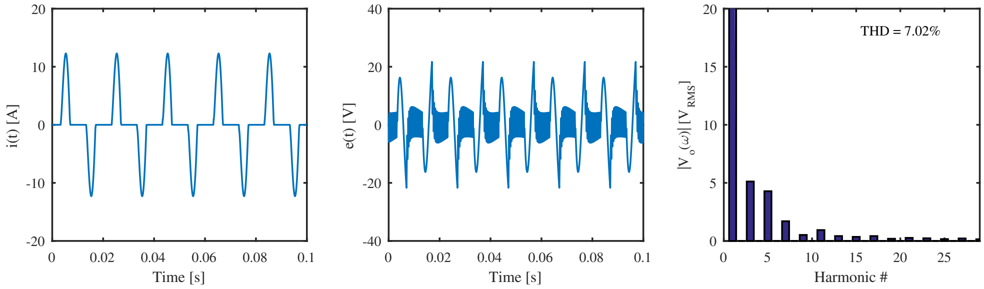

(b) 1st-order LPF

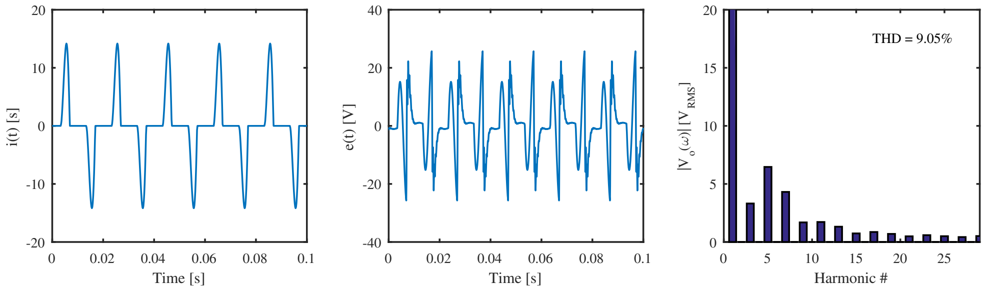

(c) 2nd-order LPF

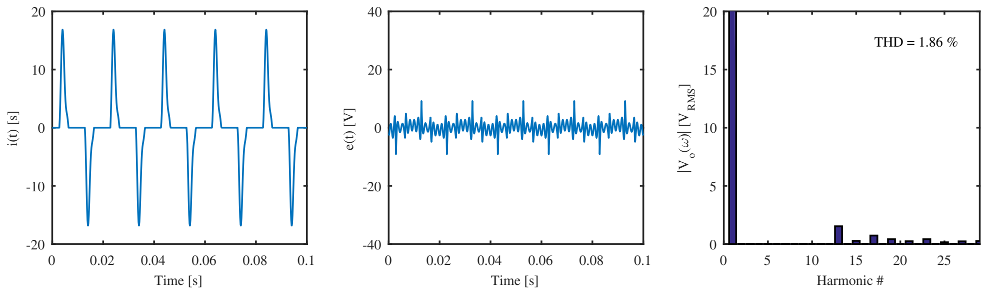

(d) The proposed FSF

Figure 8. Simulation results for UDE control utilizing different filters

Rioual, P., Pouliquen, H., and Louis, J.P. (1996). Regulation of a PWM rectifier in the unbalanced network state using a generalized model. *IEEE Trans. Power Electron.*, 11(3), 495–502.

Shendge, P. and Patre, B. (2007). Robust model following load frequency sliding mode controller based on UDE and error improvement with higher order filter. *IAENG International Journal of Applied Mathematics*, 37(1), 1–6.

Tomizuka, M. (2008). Dealing with periodic disturbances in controls of mechanical systems. *Annual Reviews in Control*, 32(2), 193–199.

Wang, Y., Ren, B., and Zhong, Q.C. (2016). Robust power flow control of grid-connected inverters. *IEEE Transactions on Industrial Electronics*, 63(11), 6887–6897.

Youcef-Toumi, K. and Ito, O. (1987). Controller design for systems with unknown nonlinear dynamics. In *Proc. of American Control Conference (ACC)*, 836–844.

Youcef-Toumi, K. and Ito, O. (1990). A time delay controller for systems with unknown dynamics. *Journal of Dyn. Sys. Meas. Con.Trans. ASME*, 112(1), 133–142.

Zhong, Q.C., Kuperman, A., and Stobart, R. (2011). Design of UDE-based controllers from their two-degree-of-freedom nature. *International Journal of Robust and Nonlinear Control*, 21, 1994–2008.

Zhong, Q.C. and Rees, D. (2004). Control of uncertain LTI systems based on an uncertainty and disturbance estimator. *Journal of Dyn. Sys. Meas. Con.Trans. ASME*, 126(4), 905–910.